VOL. 9, NO. 11, NOVEMBER 2014 ISSN 1819-6608
ARPN Journal of Engineering and Applied Sciences


www.arpnjournals.com

INTERPRETATION OF PRESSURE TESTS IN HORIZONTAL WELLS IN HOMOGENEOUS AND HETEROGENEOUS RESERVOIRS WITH THRESHOLD PRESSURE GRADIENT

Freddy Humberto Escobar[1], Yu Long Zhao[2] and Lie Hui Zhang[2]
[1]Universidad Surcolombiana/CENIGAA, Avenida Pastrana - Cra 1, Neiva, Huila, Colombia
[2]State Key Laboratory of Oil and Gas Reservoir Geology and Exploitation, Southwest Petroleum University, Xindu Street, Xindu district, Chendu, Sichuan, P. R. China
E-Mail: fescobar@usco.edu.co

ABSTRACT

A pressure gradient level that must be reached to enable the fluid to overcome the viscous forced is defined as the threshold pressure gradient, TPG. It has been observed that the TPG has effect on the pseudorradial (or late radial) flow regime of horizontal wells, but such earlier flow regimes as early radial, early linear and elliptical do not suffer the effect of the TPG. In this work, a methodology previously introduced in the literature for well test interpretation in horizontal wells drilled in both homogeneous and naturally fractured formations has been adapted by using some corrections factors. The re-formulated methodology was successfully tested on synthetic pressure tests.

Keywords: horizontal wells, TDS technique, pressure transient analysis, flow regimes.

1. INTRODUCTION

Several studies have been devoted to study the impact of the onset pressure gradient required to initiate fluid flow. Prada and Civan (1999) conducted a laboratory investigation to see the effect of the onset pressure gradient on several low permeability rock samples so empirical corrections of the minimum pressure gradient as a function of fluid mobility were developed.

Raymond and Philip (1963) reported the existence of TPG in the water flow through soils with high clay content. Pascal (1981) studied the effect of TPG on the fluid flow through a porous medium and evaluated its role on the pressure and flow rate distributions. Yun, Yu, and Cai (2008) presented a fractal model to describe the Bingham fluids flow in porous medium with the consideration of TPG based on the fractal characteristics of pores.

Regarding the influence of TPG on well pressure tests, we found the work of Lu and Ghedan (2011) presented an analytical solution to study the pressure behavior of vertical wells in low permeability reservoirs under the influence of TPG. They conducted the interpretation via the straight-line conventional analysis. Later, Lu (2012) extended the work of Lu and Ghedan (2011) to include the effect of TPG on pressure tests in uniform-flux hydraulically fractured vertical wells.

Owayed and Tiab (2008) discussed the flow of a slightly compressible Bingham fluid and developed new analytical equations based on pressure and pressure derivative behavior of horizontal wells. Zhao *et al*. (2013) presented an analytical solution for the horizontal well transient pressure behavior of a dual-porosity formation with the influence of TPG. They commented on the pressure and pressure derivative behavior and observed that the effect of TPG is seen during the pseudorradial flow regime. This work is an extension of the research presented by Zhao *et al*. (2013) to introduce correction factors of the TPG so the methodology presented by Engler and Tiab (1996a) - homogeneous case- and Engler and Tiab (1996b) - naturally-fractured dual-porosity formations- can be applied.

2. MATHEMATICAL FORMULATION

2.1. Dimensionless quantities

The dimensionless quantities considered in this study for both homogeneous and anisotropic reservoirs and naturally fracture systems are given below. The dimensionless time is given by:

$$t_D = \frac{0.0002637 k_y t}{\mu \phi c_t r_w^2} \quad (1)$$

For heterogeneous systems, the total compressibility-porosity product is changed as $(\phi c_t)_{m+f}$. The dimensionless pressure, pressure derivative, second pressure derivative and threshold pressure gradient are defined by:

$$P_D = \frac{k_y L_w \Delta P}{141.2 q \mu B} \quad (2)$$

$$t_D * P_D' = \frac{k_y L_w (t * \Delta P')}{141.2 q \mu B} \quad (3)$$

$$t_D^2 * P_D'' = \frac{k_y L_w (t^2 * \Delta P'')}{141.2 q \mu B} \quad (4)$$

$$PG_D = \frac{k_h L_w h_z PG}{141.2 q \mu B} \quad (5)$$

The dimensionless lengths:

$$L_{wD} = \frac{L_w}{h_z}\sqrt{\frac{k_z}{k_h}} \quad (6)$$

$$r_{eD} = \frac{r_e}{L_w} \quad (7)$$

2.2. Homogeneous and anisotropic reservoirs

Zhao *et al*. (2013) presented the well pressure behavior solution for a horizontal well in naturally-fractured formation which is easily extended to homogeneous formations. Both solutions become the basis of this study. Figure-1 presents the dimensionless pressure and pressure derivative behavior for a homogeneous system in which the following flow periods are chronologically recognized: wellbore storage, early radial flow regime, linear flow regime, elliptical flow regime and late-radial or pseudorradial flow regime and pseudosteady-state period. Due to the fact the system geometry is circular then no late linear flow regime is presented in such plot.

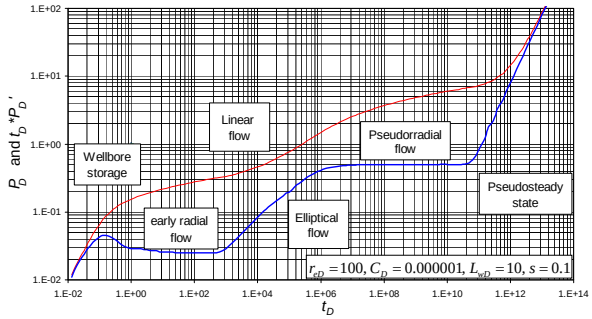

Figure-1. Dimensionless pressure and pressure derivative vs. time of a horizontal well in a closed-circular homogeneous reservoir.

Engler and Tiab (1996a) presented a methodology based upon the TDS technique, Tiab (1993) to characterize these flow regimes which are used for obtaining reservoir permeability, as follows:

The early radial flow regime provides $(k_y k_z)^{0.5}$,

$$\sqrt{k_y k_z} = \frac{70.6 q\mu B}{L_w (t*\Delta P')_{er}} \quad (8)$$

Both early linear and late linear are used to obtain, respectively, k_y, using the value of the pressure derivative on each flow regime at a time of 1 hr, extrapolated if necessary,

$$k_y = \left(\frac{4.064qB}{L_w h_z (t*\Delta P')_{L1}}\right)^2 \frac{\mu}{\phi c_t} \quad (9)$$

$$k_y = \left(\frac{4.064qB}{h_z (t*\Delta P')_{LL1}}\right)^2 \left(\frac{\mu}{\phi c_t h_x^2}\right) \quad (10)$$

The elliptical flow equation initially presented by Escobar *et al*. (2004) and later modified by Martinez, Escobar and Bonilla (2012) allows obtaining the horizontal permeability, $k_h = (k_x k_y)^{0.5}$,

$$\sqrt{k_x k_y} = \frac{5.554 q\mu^{0.64} B k_x^{0.36}}{h_z (\phi c_t)^{0.36} L_w^{0.72} (t*\Delta P')_{Ell}} t_{Ell}^{0.36} \quad (11)$$

Martinez, Escobar and Bonilla (2012) also presented the conventional straight-line methodology to characterize such flow regime. Escobar and Montealegre-M. (2008) presented also the elliptical flow characterization via conventional technique for vertical wells.

Engler and Tiab (1996a) presented the dimensionless pressure derivative solution for pseudorradial flow regime, such as,

$$t_D * P_D' = \frac{1}{2}\frac{L_w}{h_z}\sqrt{\frac{k_y}{k_x}} \quad (12)$$

Once the above expression is combined with Equation (2) allows obtaining $k_h = (k_x k_y)^{0.5}$

$$\sqrt{k_x k_y} = \frac{70.6 q\mu B}{h_z (t*\Delta P'_{pr})} \quad (13)$$

Since the dimensionless pressure derivative behavior is given by:

$$t_D * P_D' = 2\pi t_{DA} \quad (14)$$

Combination of Equations (13) and (14) leads to an equation for well drainage area estimation,

$$A = \frac{h_z \sqrt{k_x k_y}\, t_{prpi}}{301.77 L_w \phi\mu c_t} \quad (15)$$

Engler and Tiab (1996a) also provided more expressions using the intersection points formed between the different flow regimes from which only two cases considered of importance by the authors are reported here:

$$k_z = 301.77 \phi\mu c_t \frac{h_z^2}{t_{i,er-el}} \quad (16)$$

$$\frac{k_x}{L_w^2} = \frac{301.77 \phi\mu c_t}{t_{i,el-pr}} \quad (17)$$

Engler and Tiab (1996a) also found that the derivative ratios provide unique feature for the analysis. Then, the ratio between the radial flows allows for obtaining either k_x or k_z,

$$\frac{(t*\Delta P')_{er1}}{(t*\Delta P')_{pr1}} = \frac{h_z}{L_w}\sqrt{\frac{k_x}{k_z}} \quad (18)$$

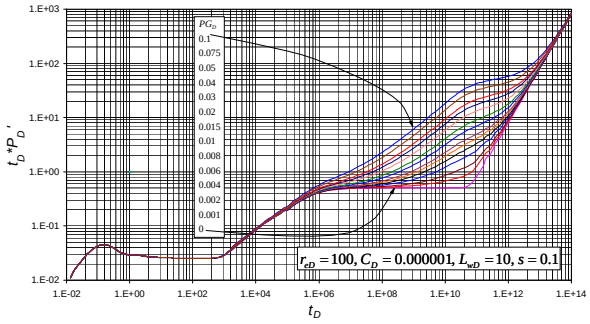

Figure-2. Dimensionless pressure derivative vs. time for different dimensionless pressure gradient values of a horizontal well in a closed-circular homogeneous reservoir.

The effect of the threshold pressure on the pressure derivative curve is observed in Figure-2 for different values of dimensionless threshold pressure covering a practical range. Notice that the early radial and early linear flows are unaffected; then, application of the *TDS* technique for such flow regimes is given by Engler and Tiab (1996a). The elliptical flow is slightly affected but the pseudorradial flow regime is strongly affected. So are late linear regime and the pseudosteady-state period. However, since the early linear flow regime is useful to provide k_y, then, there is no need of considering it in this study. It is important to see that is the pressure test in run long enough then the late time pseudosteady state will be observed.

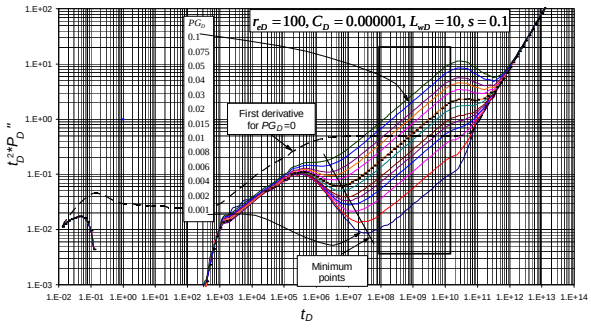

Figure-3. Dimensionless second pressure derivative vs. time for different dimensionless pressure gradient values of a horizontal well in a closed-circular homogeneous reservoir.

The starting point is trying to find out the value of the dimensionless threshold pressure which is not easily obtained from the characteristic points and lines of Figure-2. Then, the second pressure derivative, Figure-3, is considered. There, three main features are observed: (1) A maximum point after linear/elliptical flow vanishes; (2) a minimum point follows the maximum point, and (3) a 0.5-slope straight line as shown inside the square of Figure-3.

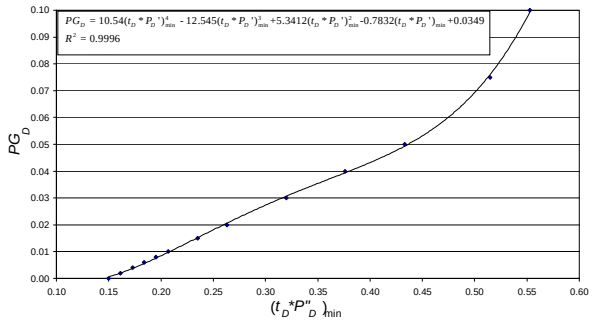

Figure-4. Correlation of the minimum dimensionless second pressure derivative with the dimensionless threshold pressure.

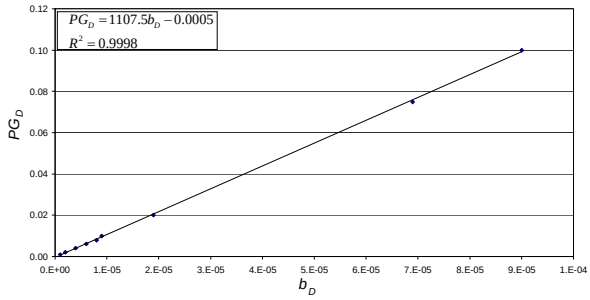

Figure-5. Correlation of the intercept of the half-slope straight line on the second pressure derivative and the dimensionless threshold pressure.

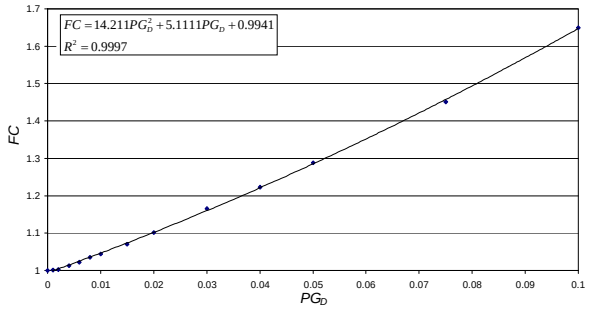

Figure-6. Correction factor of the dimensionless second pressure derivative dimensionless at which the maximum occurs - Homogeneous reservoirs.

The second pressure derivative at which the minimum point takes place; see Figure-3, correlates perfectly with the dimensionless threshold pressure,

Figure-4, from where the following correlation is obtained:

$$PG_D = 10.54(t_D * P_D')^4_{\min} - 12.545(t_D * P_D')^3_{\min} + 5.3412(t_D * P_D')^2_{\min} - 0.7832(t_D * P_D')_{\min} + 0.0349 \quad (19)$$

The above expression requires the estimation of the dimensionless second pressure derivative which is a function of k_y. The latter can be found from the early-linear flow regime, Equation (9).

For cases where the minimum point is not easy to be read, due to noisy data, it is recommended to obtain the dimensionless threshold pressure from the intercept, *b*, of the half-slope straight line (which region is enclosed in the square, Figure-4). This intercept correlates quite well with the threshold pressure as indicated in Figure-5,

$$PG_D = 1107.5 b_D - 0.0005 \quad (20)$$

Where

$$b_D = \frac{k_y L_w b}{141.2 q \mu B} \quad (21)$$

As indicated before, the dimensionless second pressure derivative displays a maximum point after the linear or elliptical flow regimes are felt as indicated in Figure-2. This maximum point is practically the same for all the given threshold pressures if a correction factor, *FC*, is applied as perfectly correlated in Figure-6. Then, at that maximum point the second derivative is given by:

$$t_D^2 * P_D'' = \frac{1}{10}\frac{L_w}{h_z}\sqrt{\frac{k_y}{k_x}} FC \quad (22)$$

The correction factor obtained from Figure-6 leads to obtained:

$$t_D^2 * P_D'' = \frac{1}{10}\frac{L_w}{h_z}\sqrt{\frac{k_y}{k_x}}(14.211 PG_D^2 + 5.1111 PG_D + 0.9941) \quad (23)$$

After replacing Equation (4) into the above expression, it yields:

$$\sqrt{k_x k_y} = \frac{14.12 q \mu B (14.211 PG_D^2 + 5.1111 PG_D + 0.9941)}{h_z (t^2 * \Delta P''_{pr\_\max})} \quad (24)$$

Once the horizontal permeability is estimated then the actual value of the radial pressure derivative, $(t*\Delta P')_{pr}$ is obtained from Equation (13). This value corresponds to a horizontal straight line which may be drawn on the pressure derivative plot so its intersection with the late pseudosteady state line will provide the horizontal ell drainage area using Equation (15).

The effective wellbore length must be at least 5 times higher than the formation thickness for the early linear flow regime to develop; spherical flow will be observed, otherwise. Figure-7 shows such behavior. Since linear flow is unknown, then the procedure outlined before does not apply. For such cases it is recommended to assume isotropic system and assume the value of the pseudorradial derivative (horizontal line), then, the following expression applies;

$$\frac{h_z}{L_w}\sqrt{\frac{k_h}{k_z}} = \frac{3.9442\times10^{-4} + 0.956868x - 0.8434x^2}{1 - 1.04747x + 0.094568x^2} \quad (25)$$

where

$$x = \frac{(t * \Delta P')_{\min}}{(t * \Delta P')_{pr}} \quad (26)$$

Expression 26 was original introduced by Engler and Tiab (1996a) as a graphical correlation.

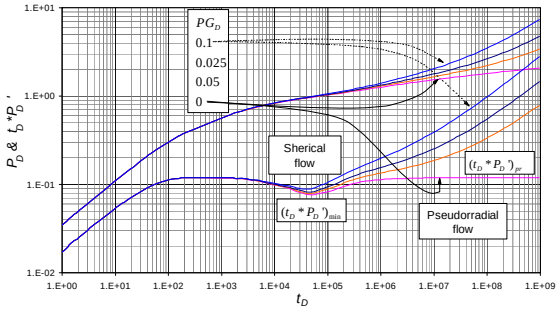

Figure-7. Dimensionless pressure and pressure derivative vs. time behavior for a horizontal well with L_D = 0.5 and different threshold pressure values.

2.3. Naturally fractured reservoirs

The expressions for the estimation of permeabilities in homogeneous systems are applied here, so in this section we will focused on obtaining the Warren-and-Root parameters, ω and $\underline{\lambda}$, Warren and Root (1963).

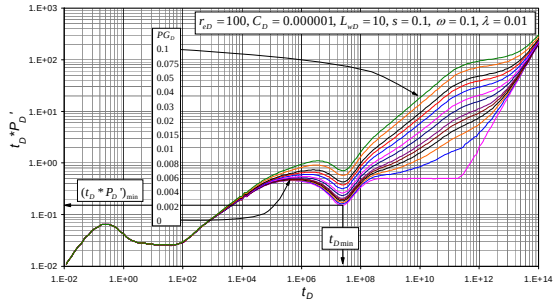

Figure-8. Dimensionless pressure derivative vs. time for different dimensionless pressure gradient values of a horizontal well in a closed-circular heterogeneous reservoir.

Figure-8 shows the dimensionless pressure derivative vs. time log-log plot for a naturally fractured reservoir subjected to variations of threshold pressure gradient which effect takes place during the pseudorradial flow regime. For large values of the interporosity flow parameter the trough appears before the pseudorradial flow regime, then, the methodology outlined by Engler and Tiab (1996b) applies. Three main characteristics are seen in Figure-8; (1) An unchanging time at which the trough takes place, although, the minimum pressure derivative is affected by the threshold pressure, (2) the unit-slope line occurring after the minimum point keeps unaffected. Then, the point of intersection of the second radial flow regime (after the unit-slope line) with such line is also unaltered, and (3) the slope of the second radial flow regime is a function of the threshold pressure as described by Figure-9. The governing expression is then:

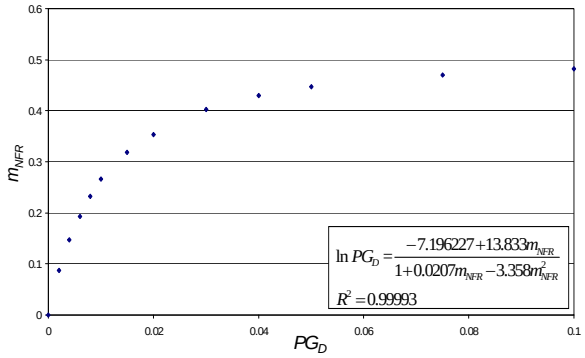

Figure-9. Correlation between the PG_D and the slope of the second radial flow regime.

$$\ln PG_D = \frac{-7.196227+13.833m_{NFR}}{1+0.0207m_{NFR}-3.358m_{NFR}^2} \quad (27)$$

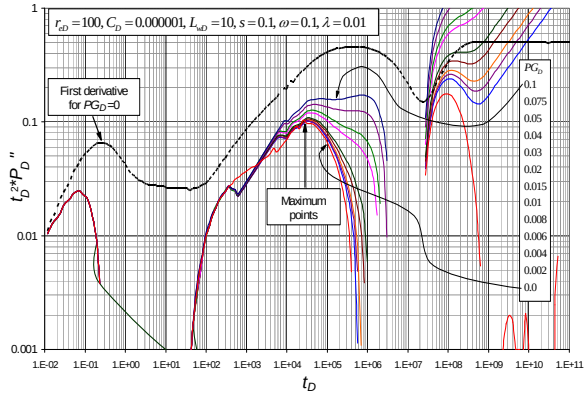

Figure-10. Dimensionless second pressure derivative vs. time for different dimensionless pressure gradient values of a horizontal well in a closed-circular heterogeneous reservoir.

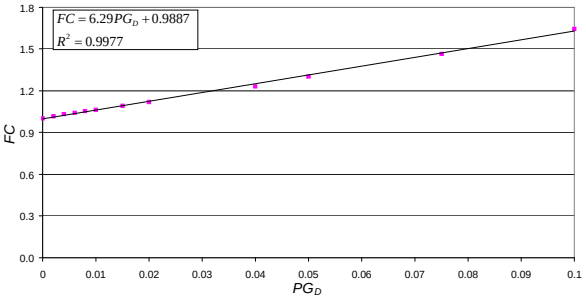

Figure-11. Correction factor of the dimensionless time at which the maximum second pressure derivative occurs – Naturally fractured reservoirs.

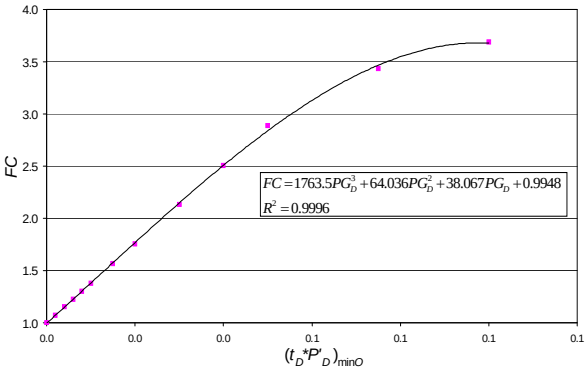

Figure-12. Correction factor of the minimum dimensionless pressure derivative.

As observed in Figure-10, once linear/elliptical flow vanishes, the second pressure derivative displays a maximum point which after corrected is then used to obtained the horizontal permeability; such correlation is obtain from Figure-11,

$$t_D^2 * P_D'' = 0.0971 \frac{L_w}{h_z}\sqrt{\frac{k_y}{k_x}}FC \quad (28)$$

$$t_D^2 * P_D'' = 0.0971 \frac{L_w}{h_z}\sqrt{\frac{k_y}{k_x}}(6.29PG_D + 0.9887) \quad (29)$$

After replacing Equation 4 into Equation 29, it yields:

$$\sqrt{k_x k_y} = \frac{q\mu B(86.2392PG_D + 13.5556)}{h_z(t^2 * \Delta P'')_{max}} \quad (30)$$

Engler and Tiab (1996b) presented several expressions to determine the dimensionless storativity coefficient, ω, and the interporosity flow parameter, λ, using such characteristics points as the minimum time and pressure derivative taking place at the trough, the pseudorradial flow regime pressure derivative and the intercept between the unit-slope line (if seen) and the radial flow regime.

$$\omega = 0.15866\left\{\frac{(t*\Delta P')_{\min}}{(t*\Delta P')_{er}}\right\} + 0.54653\left\{\frac{(t*\Delta P')_{\min}}{(t*\Delta P')_{er}}\right\}^2 \quad (31)$$

$$\lambda = \frac{42.5 L_w (\phi c_t)_{f+m} r_w^2}{q\,B}\left(\frac{t*\Delta P'}{t}\right)_{\min} \quad (32)$$

$$\omega = 0.18174(\lambda \cdot t_{D,\min}) + 0.22339(\lambda \cdot t_{D,\min})^2 + 2.1558(\lambda \cdot t_{D,\min})^3 \quad (33)$$

When the transition period occurs after the onset of the early linear flow regime, the interporosity flow parameter can be obtained from the ratio of the maximum and minimum pressure derivatives,

$$\log(1/\lambda) = 3.3467 + 10.720\left(\frac{(t*\Delta P')_{\max}}{(t*\Delta P')_{pr}}\right) - 15.758\left(\frac{(t*\Delta P')_{\max}}{(t*\Delta P')_{pr}}\right)^2 + 10.472\left(\frac{(t*\Delta P')_{\max}}{(t*\Delta P')_{pr}}\right)^3 \quad (34)$$

Equations 31 to 34 can also be applied if the value of the minimum pressure derivative is corrected. Coming back to Figure-8, we observe that the minimum point occurs at the same time but the pressure derivative changes as a function of the threshold pressure gradient. Such correlation is given in Figure-12 which allows finding,

$$(t_D*P_D')_{\min} = \frac{(t_D*P_D')_{\min O}}{1763.5PG_D^3 + 64.036PG_D^2 + 38.067PG_D + 0.9948} \quad (35)$$

Also, the point of intersection between the pseudorradial flow regime in the homogeneous region (second radial flow regime) and the unit-slope line taking place in the transition period leads to obtain the interporosity flow parameter,

$$\lambda = \left(\frac{(\phi c_t)_{f+m}\,\mu r_w^2}{0.0002637\sqrt{k_x k_y}}\right)\frac{1}{t_{us,i}} \quad (36)$$

Finally, we did not elaborate on the determination of the skin factors; however, it can be determined by modifying the original expression of Engler and Tiab (1996b) with an analogy taken from Equation (78) of Lu and Ghedan (2011).

$$s_m + s_z = \frac{L_w}{2h_z}\sqrt{\frac{k_z}{k_y}}\left[\frac{\Delta P_{pr} + PG(r_w)}{(t*\Delta P')_{pr}} - \ln\left(\frac{k_x t_{pr}}{\phi\mu c_t L_w^2}\right) + 4.659\right] \quad (37)$$

Table-1. Relevant data for example-1.

	Value	
Parameter	**Example-1**	**Example-2**
k_x, md	400	5
k_y, md	100	5
k_z, md	100	20
r_w, ft	0.5	0.5
L_w, ft	1500	750
h_z, ft	50	50
q, BPD	300	300
μ, cp	5	2.2
ϕ, %	10	10(*)
B, rb/STB	1.1	1.
c_t, 1/psi	$1x10^{-5}$	$1x10^{-4}$(*)
r_{eD}	30	
PG_D	0.01	0.006
λ	1	$1x10^{-8}$
ω	0	0.05

(*) includes matrix plus fractures

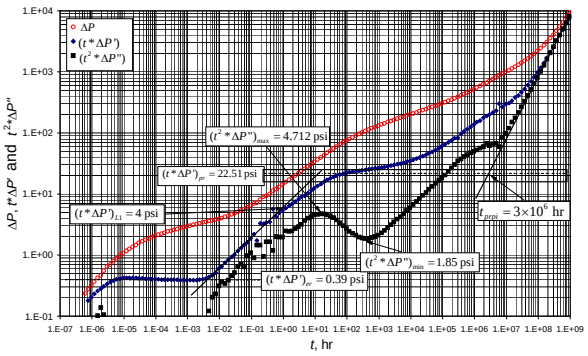

Figure-13. Pressure, pressure derivative and second pressure derivative versus time for example 1.

3. EXAMPLES

3.1. Homogeneous reservoir synthetic example

The pressure drop, pressure derivative and second pressure derivative versus time test reported in Figure-13 was generated using the input data given in the second column of Table-1. It is required to characterize this test.

Solution. The following information was read from Figure-13,

$(t*\Delta P')_{er}$ = 0.39 psi
$(t*\Delta P')_{L1}$ = 4 psi
$t_{prpi} = 3x10^6$ hr
$(t^2*\Delta P")_{\max}$ = 4.712 psi
$(t^2*\Delta P")_{\min}$ = 1.85 psi

The procedure is outlined as follows:

a) Find $(k_y k_z)^{0.5}$ with Equation (8). Result 396.82 md$^{0.5}$
b) Find k_y from Equation (9). Result 99.92 md
c) By combining results from steps 1 and 2, k_z = 19.12 md
d) Equation (4) is used to find $(t_D{}^2 * P_D{}')_{min}$ = 0.0397 psi
e) Find the dimensionless threshold pressure with Equation (19). Result 0.0115 ≅ 0.01.
f) The correction factor given in Equation (22) is estimated by the correlation given in Figure-6. Result 1.0466
g) Find $(k_x k_y)^{0.5}$ with Equation (24). Result 98.89 md
h) Knowing k_y find k_x. Result 97.864 md.
i) With the value of step 7, find $(t*\Delta P')_{pr}$ using Equation 13. Result 22.503 psi
j) Draw a horizontal line along the value of step 9, corresponding to the pseudorradial flow regime for the zero threshold pressure. This line has been enclosed inside a rectangle (for pedagogical purposes)
k) Draw the unit-slope line corresponding to the late-time pseudosteady-state period and read the intercept of this line with the pseudorradial flow regime
l) Find the well drainage area with Equation (15). Result 157473 acres with corresponds to a radius of 46727.3 ft or r_{eD} = 31.15

Note: alternatively, k_z and k_x can be estimated with Equation 15 and 16, respectively. Also, elliptical flow is observed approximately at 1 hr which can be sued to estimate $(k_x k_y)^{0.5}$.

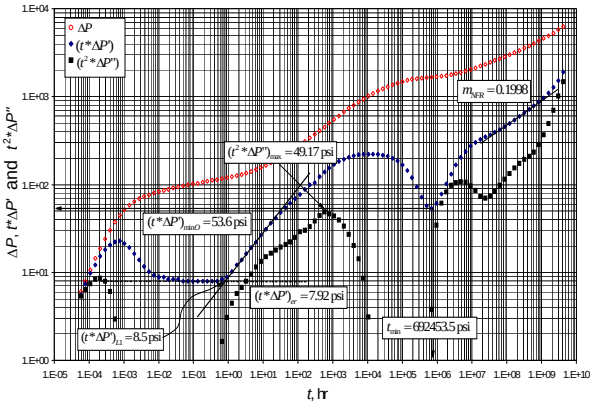

Figure-14. Pressure, pressure derivative and second pressure derivative versus time for example 2.

3.2. Heterogeneous reservoir synthetic example

Figure-14 presents synthetic data of pressure, pressure derivative and second pressure derivative versus time generated with the information given in the third column of Table-1. Find permeability, dimensionless threshold pressure and the naturally-fractured reservoir parameters.

Solution. The following information was read from Figure-14,

$(t*\Delta P')_{er}$ = 7.92 psi $(t*\Delta P')_{L1}$ = 8.5 psi
$(t^2*\Delta P")_{max}$ = 49.17 psi $(t^2*\Delta P')_{minO}$ = 53.6 psi
t_{min} = 692453.5 psi

The procedure is outlined as follows:

a) Find $(k_y k_z)^{0.5}$ with Equation (8). Result 9.806 md$^{0.5}$
b) Find k_y from Equation (9). Result 5.03 md
c) By combining results from steps 1 and 2, k_z = 19.11 md
d) Find the dimensionless threshold pressure with Equation (27). Result 0.0061 ≅ 0.006.
e) Find $(k_x k_y)^{0.5}$ with Equation (30). Result 4.73 md
f) Knowing k_y find k_x. Result 4.44 md.
g) With the value of step 5, find $(t*\Delta P')_{pr}$ using Equation 13. Result 246.52 psi. If wanted draw a horizontal line along this value, corresponding to the pseudorradial flow regime for the zero threshold pressure. In this case is not needed since there is no late pseudosteady state period.
h) Find $\omega\lambda$ with Equation (31). Result 0.045
i) Find λ with Equation (32). Result 1.34x10^{-8}.

Note: alternatively, k_z and k_x can be estimated with Equation 15 and 16, respectively. Also, elliptical flow is observed approximately at 20 hr which can be sued to estimate $(k_x k_y)^{0.5}$. Equations (33) and (34) can also be used to re-estimate ω and λ.

4. COMMENTS ON THE RESULTS

The agreement between the simulated and estimated results in the worked examples show that the correction factors introduced in this study allow for the application of the interpretation methodology introduced by Engler and Tiab (1996a, 1996b).

5. CONCLUSIONS

The interpretation methodology introduced by Engler and Tiab (1996a, 1996b) were extended for the case of pressure tests affected by the threshold gradient by including some correction factors which are found from characteristic points and lines found on the pressure, pressure derivative and second pressure derivative vs. time log-log plot. The corrections factors were successfully applied to synthetic examples.

ACKNOWLEDGEMENTS

The authors gratefully thank the Most Holy Trinity and the Virgin Mary mother of God for all the blessing received during their lives.

Nomenclature

b	Slope
B	Volumetric factor, rb/Mscf
c_t	System total compressibility, 1/psi
FC	Correction factor
k	Permeability, md
k_h	Horizontal permeability, $(k_x k_y)^{0.5}$
h_z	Reservoir thickness, ft
h_x	Reservoir length, ft
L_w	Effective horizontal wellbore length, psi
P	Pressure, psi
PG	Threshold pressure gradient, psi/ft
PG_D	Dimensionless threshold pressure gradient
P_{wf}	Bottomhole flowing pressure, psi
r	Radius, ft
s	Skin factor
t	Time, hr
t_D	Dimensionless time
$t*\Delta P'$	Pressure derivative, psi
$t^2*\Delta P''$	Second pressure derivative, psi
t_D*P_D'	Dimensionless pressure derivative
$t_D^2*P_D''$	Dimensionless second pressure derivative, psi

Greeks

ϕ	Porosity, fraction
λ	Interporosity flow parameter
μ	Viscosity, cp
ω	Dimensionless storativity coefficient

Suffices

e	External
D	Dimensionless
DA	Dimensionless based on drainage area
el	Early linear
i,el-pr	Early linear and pseudorradial intercept
i,er-el	Early radial and early linear intercept
er	Early radial
ELL	Elliptical
f	Fracture
h	Horizontal
i	Initial
*L*1	Early linear at 1 hr
*LL*1	Late linear at 1 hr
m	Matrix, slope, mechanical
max	Maximum
min	Minimum
minO	Observed minimum
NFR	Naturally fractured reservoir
p	Pseudosteady state
pr	Pseudorradial
prpi	Pseudorradial-Pseudosteady intersection
us,i	Transition unit-slope and pseudorradial intercept
x	Direction in the *x*-axis
y	Direction in the *y*-axis
w	Well
z	Direction in the *z*-axis

REFERENCES

Engler T. W. and Tiab D. 1996a. Analysis of Pressure and Pressure Derivatives without Type-Curve Matching. 6-Horizontal Well Tests in Anisotropic Reservoirs. Jour. Petr. Sci. and Eng. 15: 153-168.

Engler T. W. and Tiab D. 1996b. Analysis of Pressure and Pressure Derivatives without Type-Curve Matching. 5-Horizontal Well Tests in Naturally Fractured Reservoirs. Jour. Petr. Sci. and Eng. 15: 139-151.

Escobar F.H., Muñoz O.F. and Sepúlveda J.A. 2004. Horizontal Permeability Determination from the Elliptical Flow Regime for Horizontal Wells. CT and F - Ciencia, Tecnología y Futuro. 2(5): 83-95.

Escobar F.H. and Montealegre-M M. 2008. Determination of Horizontal Permeability from the Elliptical Flow of Horizontal Wells Using Conventional Analysis. Journal of Petroleum Science and Engineering. 61: 15-20.

Lu J. and Ghedan S. 2011. Pressure behavior of vertical wells in low-permeability reservoirs with threshold pressure gradient. Special Topics and Reviews in Porous Media. 2(3): 157-169.

Lu J. 2012. Pressure behavior of uniform-flux hydraulically fractured wells in low-permeability reservoirs with threshold pressure gradient. Special Topics and Reviews in Porous Media - An International Journal. 3(4): 307-320.

Martinez J.A., Escobar F.H. and Bonilla L.F. 2012. Reformulation of the Elliptical Flow Governing Equation for Horizontal Wells. Journal of Engineering and Applied Sciences. 7(3): 304-313.

Owayed J.F. and Tiab. D. 2008. Transient pressure behavior of Bingham non-Newtonian fluids for horizontal wells Journal of Petroleum Science and Engineering. 61: 21-32.

Pascal H. 1981 Nonsteady flow through porous media in the presence of a threshold gradient. Acta Mechanica. 39: 207-224.

Raymond J. M. and Philip F. L. 1963. Threshold Gradient for water flow in clay systems Soil Science Society of America Journal. 27: 605-609.

Tiab D. 1993. Analysis of Pressure and Pressure Derivative without Type-Curve Matching: 1- Skin and Wellbore Storage. Journal of Petroleum Science and Engineering. 12: 171-181.

Warren J.E. and Root P.J. 1963. The Behavior of Naturally Fractured Reservoirs. SPEJ. pp. 245-255.

Yun M. J., Yu B.M. and Cai J.C. 2008. A fractal model for the starting pressure gradient for Bingham fluids in porous media International Journal of Heat and Mass Transfer. 51: 1402-1408.

Zhao Y.L., Zhang L.H., Feng W. Zhang B.N and Lis Q.G. 2013. Analysis of horizontal well pressure behavior in fractured low permeability reservoirs with consideration of the threshold pressure gradient. Journal of Geophysics and Engineering. 10: 1-10.